AMERICAN SOCIETY FOR MICROBIOLOGY | Molecular and Cellular Biology®

RESEARCH ARTICLE

A Key Regulator of Cell Adhesion: Identification and Characterization of Important *N*-Glycosylation Sites on Integrin α5 for Cell Migration

Qinglei Hang,[a] Tomoya Isaji,[a] Sicong Hou,[a] Yuqin Wang,[a,b] Tomohiko Fukuda,[a] Jianguo Gu[a,b]

Division of Regulatory Glycobiology, Institute of Molecular Biomembrane and Glycobiology, Tohoku Medical and Pharmaceutical University, Sendai, Miyagi, Japan[a]; Department of Pharmacology, Pharmacy College, Nantong University, Nantong, Jiangsu, China[b]

ABSTRACT The *N*-glycosylation of integrin $\alpha5\beta1$ is thought to control many fundamental aspects of cell behavior, including cell adhesion and migration. However, the mechanism of how *N*-glycans function remains largely obscure. Here, we used a loss-of-function approach. Wild-type (WT) integrin $\alpha5$ and *N*-glycosylation mutant S3-5 (sites 3 to 5) integrin $\alpha5$, which contains fewer *N*-glycans, were stably reconstituted in $\alpha5$ knockout cancer cells. We found that the migration ability of S3-5 cells was decreased in comparison with that of the WT. Interestingly, the levels of phosphorylated focal adhesion kinase and actin stress fiber formation were greatly enhanced in the S3-5 mutant. In a mechanistic manner, the internalization of active but not total integrin $\alpha5\beta1$ was inhibited in S3-5 cells, which is a process that is related to the enhanced expression of active integrin $\alpha5\beta1$ on the cell surface. Importantly, restoration of *N*-glycosylation on the β-propeller domain of $\alpha5$ reinstated the cell migration ability, active $\alpha5\beta1$ expression, and internalization. Moreover, these *N*-glycans are critical for $\alpha5$–syndecan-4 complex formation. These findings indicate that *N*-glycosylation on the β-propeller domain functions as a molecular switch to control the dynamics of $\alpha5\beta1$ on the cell surface that in turn is required for optimum adhesion for cell migration.

KEYWORDS *N*-glycan, activation, complex formation, internalization

Received 11 October 2016 **Returned for modification** 3 November 2016 **Accepted** 29 January 2017

Accepted manuscript posted online 6 February 2017

Citation Hang Q, Isaji T, Hou S, Wang Y, Fukuda T, Gu J. 2017. A key regulator of cell adhesion: identification and characterization of important *N*-glycosylation sites on integrin α5 for cell migration. Mol Cell Biol 37:e00558-16. https://doi.org/10.1128/MCB.00558-16.

Address correspondence to Jianguo Gu, jgu@tohoku-mpu.ac.jp.

Cell migration is essential not only for normal physiological processes such as embryonic development and wound healing but also for pathological changes such as inflammatory disease and cancer (1). Integrin, the $\alpha\beta$ heterodimeric transmembrane receptor, plays a central role in cell migration by connecting an extracellular matrix (ECM) to the cytoskeleton as well as functioning as a bidirectional signaling molecule that transmits information across the cell membrane (2). Due to its importance, integrin has been highly implicated in the development of tumor malignancy. Therefore, a detailed molecular understanding of the mechanisms involved in integrin-mediated tumor cell migration is very important for our ability to intervene in the procession of cancer.

In mammals, different α and β subunit combinations make up a total of 24 integrins. Integrins are found in either active or inactive conformations with respect to their high or low affinity for their ECM ligands (3), and an allosteric change that favors high affinity can be induced by either cytoplasmic events ("inside-out" activation) or extracellular factors ("outside-in" activation) (4), which triggers integrin clustering, cytoskeletal remodeling, and the assembly of cell adhesion complexes, including focal adhesion (FA) and fibrillary adhesion (5). Indeed, cell migration is a highly dynamic process that

is regulated by FA turnover in a coordinated manner, which requires the upregulation of cell matrix attachment at the leading edge of the cell and downregulation at its trailing edge. An appropriate balance in the adhesion and de-adhesion of the integrins is important for cell migration. The disassembly of FA requires the internalization of integrins that are either then recycled back to the cell membrane at the leading edge of migrating cells or degraded in the lysosome (6, 7). Thus, elucidating the precise mechanisms that control the internalization of integrins is fundamental to understanding coordinated cell migration.

Current insight into this regulation is derived largely from studies focused on the inner membrane, particularly cytoplasmic tails. For example, NPxY motif-binding proteins such as talin and kindlin (8), different small GTPases such as Rab and Rho families and their regulators, as well as serine/threonine kinases have been implicated in the internalization of integrins (9). However, little is known about the function of the outer membrane of integrins in this process.

Of note, integrins are known to be major glycan-carrying proteins. In fact, the functions of integrins are also dependent on their complex *N*-glycosylation modifications (10). Among the different types of integrins, $\alpha5\beta1$, a major fibronectin (FN) receptor, is believed to be a relatively well-characterized example, and *N*-glycosylation is important for its mediated many biological functions such as cell adhesion and migration (11, 12). Although the importance of the *N*-glycosylation of $\alpha5\beta1$ for cell migration has been highlighted, most studies have examined only total changes by displaying or masking specific glycan epitopes via the overexpression and knockdown, or knockout, of glycogenes. For instance, alterations in the oligosaccharide portion of integrin $\alpha5\beta1$ from the enhanced expression of some glycosyltransferase genes such as *N*-acetylglucosaminyltransferase V (GnT-V), GnT-III, or $\alpha2,6$-galactoside sialyltransferase 1 (ST6GAL1) can be used to regulate cell spreading and migration onto FN (10, 13, 14). However, the use of these approaches makes it quite difficult to clarify the details of the underlying mechanisms involved in the importance of *N*-glycosylation on $\alpha5\beta1$.

To resolve these issues using the *N*-glycosylation mutants of integrin $\alpha5$, we first identified the individual *N*-glycosylation of $\alpha5$ as a key regulator for cell migration. We found that the *N*-glycosylation of the β-propeller domain on $\alpha5$ was essential for the internalization of active integrin $\alpha5\beta1$ and membrane complex formation (e.g., syndecan-4), which in turn was important for its expression on the cell surface, which may result in a form of cell adhesion that is more appropriate for migration.

RESULTS

***N*-Glycosylation on integrin $\alpha5$ is required for $\alpha5\beta1$-mediated cell migration.** Given the importance of $\alpha5$ for cell migration, we hypothesized the involvement of *N*-glycosylation. To test this idea, we chose MDA-MB-231, HeLa, and, U-251MG cells as the cell models, which relatively express higher levels of endogenous integrins on the cell surface, including integrins $\alpha3$, $\alpha5$, $\alpha6$, αV, $\beta1$, and $\beta4$, than do 293T cells (see Fig. S1A in the supplemental material). First, we transfected either green fluorescent protein (GFP)-tagged wild-type (WT) or S3-5 mutant integrin $\alpha5$ into $\alpha5$ knockout ($\alpha5$-KO)-MDA-MB-231, $\alpha5$-KO-HeLa, and $\alpha5$-KO-U-251MG cells, which was established previously (15), because *N*-glycosylation on sites 3 to 5 (Fig. 1A) from among the 14 potential *N*-glycosylation sites in integrin $\alpha5$ is necessary for its dimer formation with $\beta1$ and total cell surface expression in CHO-B2 cells (12). Consistently, in immunoprecipitation (IP) and flow cytometric analyses, WT-MDA-MB-231 and S3-5-MDA-MB-231 cells exhibited comparable $\alpha5\beta1$ heterodimeric formation abilities (Fig. 1B) and the same expression levels of $\alpha5\beta1$ (Fig. 1C) or $\alpha5$ (Fig. S1B) on the cell surface, as did HeLa and U-251MG cells (Fig. S1C and D). It is noteworthy that due to the heterogeneity of glycans, WT $\alpha5$ on SDS-PAGE gels usually shows a diffuse band, as shown in Fig. 1B, which seems to have a relatively higher intensity than that of the S3-5 mutant. However, after the removal of heterogeneity by treatment with the peptide:*N*-glycosidase F (PNGase F) for deglycosylation, WT cells exhibited an expression level of $\alpha5$ similar to that of S3-5 mutant cells (Fig. S1E). Together, these results suggested that S3-5 mutant $\alpha5$ can also

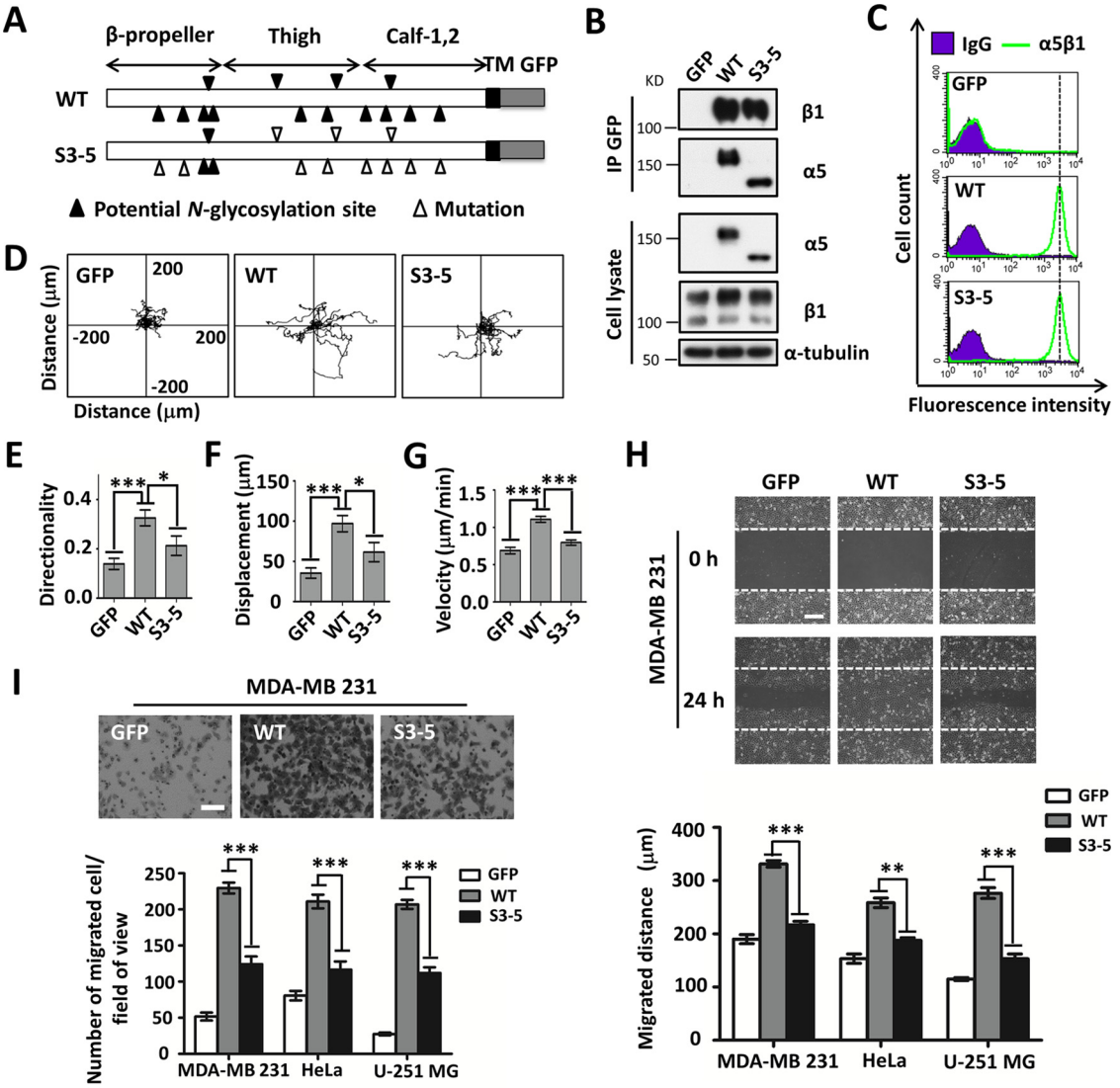

FIG 1 Comparison of FN-mediated cell migration in cell lines expressed with WT or S3-5 mutant α5. (A) Schematic diagram of potential *N*-glycosylation sites on the WT and S3-5 integrin α5 subunits. Putative *N*-glycosylation sites (N84Q, N182Q, N297Q, N307Q, N316Q, N524Q, N530Q, N593Q, N609Q, N675Q, N712Q, N724Q, N773Q, and N868Q) and point mutations are indicated. TM, transmembrane. (B and C) WT- and S3-5-MDA-MB-231 cells exhibit comparable $\alpha5\beta1$ heterodimer formation abilities (B) and the same expression levels of total integrin $\alpha5\beta1$ on the cell surface (C). (B, top) The stable cell lines were established as described in Materials and Methods. The indicated cell extracts were immunoprecipitated (IP) with anti-GFP–agarose, followed by anti-$\beta1$ and $\alpha5$ antibodies for Western blotting. (Bottom) Whole-cell extracts were also subjected to Western blotting (as an input). (C) The expression levels of $\alpha5\beta1$ were analyzed by flow cytometry. IgG was used as a control. (D to G) Individual migration tracks, persistence values, and mean speeds of GFP-, WT-, and S3-5-MDA-MB-231 cells migrating on FN. (E) Movements of the indicated cells were observed by time-lapse video microscopy ($n = 12$, from triplicate experiments). (E to G) The directionality (E), displacement (F), and speed (G) of migration were extracted from the track plots. (H and I) Cell wound closure (H) and abilities of migration toward FN (I) were determined by using wound healing and Transwell assays. Representative images of MDA-MB-231 cells appear at the top. The migrated distances relative to 0 h (H) and the numbers of migrated cells (I) of the MDA-MB-231, HeLa, and U-251MG cell lines were measured and statistically analyzed, respectively (bottom, $n = 3$ individual experiments). All values are reported as the means ± SE (error bars), as determined by Student's *t* test. *, $P < 0.05$; **, $P < 0.01$; ***, $P < 0.001$. Bars, 250 μm (H) and 350 μm (I).

serve as a successful loss-of-function model to identify the roles of the remaining *N*-glycosylation on α5 in MDA-MB-231, HeLa, and U-251MG cells.

Next, we compared cell movement on FN between GFP-, WT-, and S3-5-MDA-MB-231 cells via time-lapse imaging for 12 h (Fig. 1D). As shown in Fig. 1D to G, GFP control cells still exhibited some cell motilities, which might be due to the function of other FN receptors such as integrin $\alpha V\beta1$, but these motilities were much weaker than those of WT cells, as reflected by the directionality (Fig. 1E), displacement (Fig. 1F), and mean migration speed (Fig. 1G). Interestingly, although the cell motility of S3-5 cells was

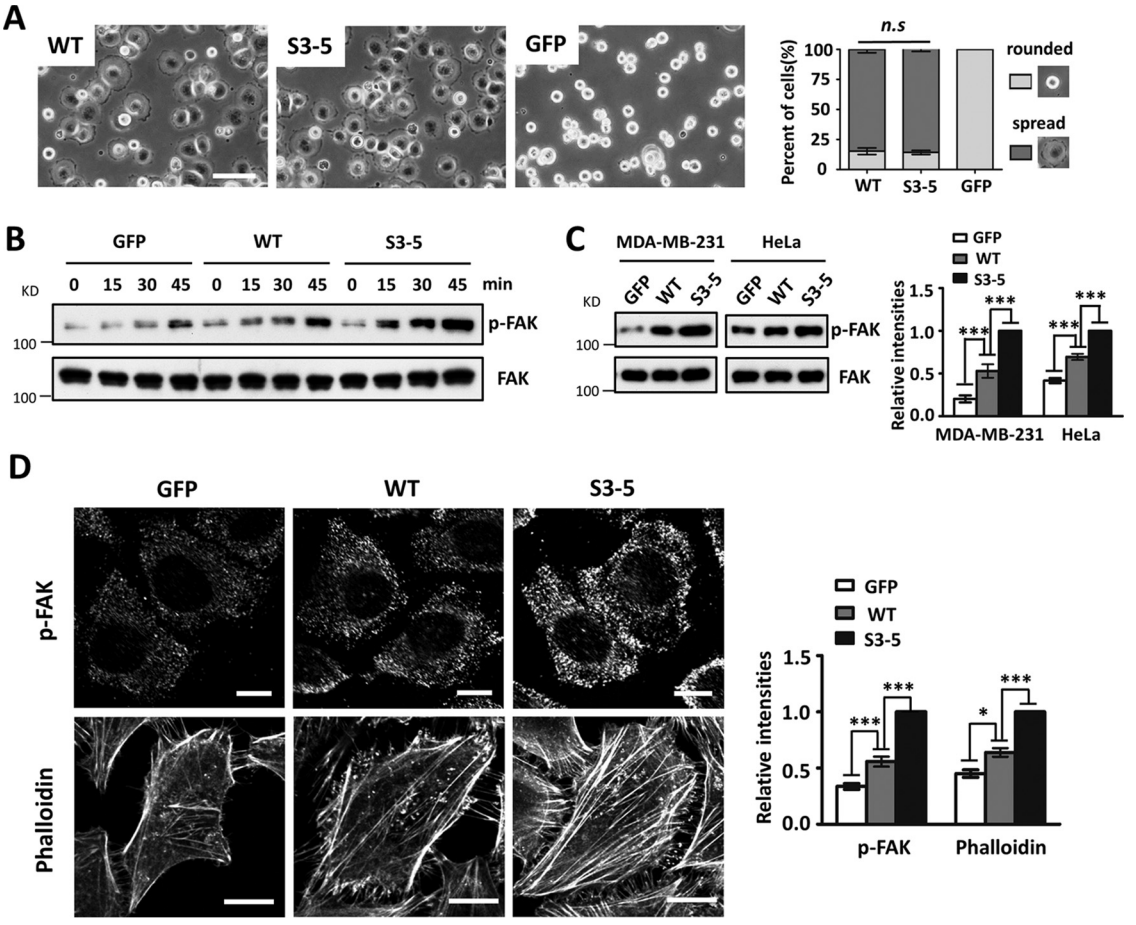

FIG 2 Changes in cell spreading, phosphorylation of FAK, and actin filament formation in S3-5 cells. (A) MDA-MB-231 cells were detached, blocked, and then replated onto FN-coated plates. After incubation for 20 min, cells were fixed, and representative images were taken. The percentages of rounded and spread cells were statistically analyzed (right) ($n = 9$, from 3 individual experiments). (B) MDA-MB-231 cells were detached, suspended in assay medium for 40 min, and then replated onto an FN-coated plate for the indicated times. Western blotting was performed with the indicated antibodies. (C, left) After culture on FN-coated dishes for 2 days, the indicated MDA-MB-231 and HeLa cells were lysed and immunoblotted with the indicated antibodies. (Right) Relative ratios (p-FAK versus FAK) ($n = 3$ individual experiments); the relative ratio was 1.0 for S3-5 mutant cells. (D) Immunofluorescence labeling and confocal microscopy of p-FAK (top) and actin stress fibers (bottom) in GFP, WT, and S3-5 mutant cells. MDA-MB-231 and HeLa cells were cultured on FN-coated coverslips, and cells were fixed, permeabilized, and then visualized with p-FAK and phalloidin-Alexa Fluor 549 (actin), respectively. The relative fluorescence intensities of p-FAK and phalloidin were quantified by using ImageJ software ($n = 6$, from 3 individual experiments); relative fluorescence intensity was 1.0 for S3-5 mutant cells. All values are reported as the means ± SE (error bars), as determined by Student's *t* test. n.s, not significant ($P > 0.05$); *, $P < 0.05$; ***, $P < 0.001$. Bars, 120 μm (A) and 20 μm (D).

stronger than that of control GFP cells, it was significantly weaker than that of WT cells (Fig. 1D to G). These phenomena were also confirmed via wound healing (Fig. 1H) and Transwell (Fig. 1I) assays. In addition, decreased wound closure (Fig. 1H, bottom) and migration abilities (Fig. 1I, bottom) were also observed for both S3-5-HeLa and S3-5-U-251MG cells. Of note, we previously showed that *N*-glycosylation on the calf domain of α5 exhibited an inhibitory effect on cell proliferation via complex formation with epidermal growth factor receptor (EGFR) (15). Taken together, these results strongly suggest that the remaining *N*-glycosylation, other than that on sites 3 to 5 of α5, plays a crucial role in the mediation of cell migration.

Deletion of *N*-glycosylation on integrin α5 increases cell matrix adhesion. In order to explore the underlying mechanisms involved in the *N*-glycosylation of α5-mediated cell migration, we compared the cell spreading abilities of WT and S3-5 cells. As shown in Fig. 2A, both WT- and S3-5-MDA-MB-231 cells exhibited comparable abilities for cell spreading on FN. A similar result was also observed for HeLa or U-251MG cells (data not shown), indicating that the remaining *N*-glycosylation on integrin α5 had no significant effect on cell spreading.

It is well known that integrin $\alpha5\beta1$ facilitates cell migration, which in turn requires a dynamic turnover of cell matrix associations, during which the activation of focal adhesion kinase (FAK) is an important step (16). To determine whether *N*-glycosylation on α5 affected the FN-mediated activation of FAK, serum-starved cells were replated onto FN-coated plates and then harvested at the indicated times. The phosphorylation levels of FAK (p-FAK) in the cell lysates were detected. As expected, Western blot (WB) analysis revealed that the levels of p-FAK upon FN stimulation at each time point in GFP-MDA-MB-231 cells were lower than those in WT cells (Fig. 2B). However, intriguingly, S3-5-MDA-MB-231 cells exhibited increased expression levels of p-FAK compared with the WT ones (Fig. 2B). In addition, when cells were grown on FN-coated dishes for 2 days, p-FAK levels were still significantly higher in S3-5 cells than those in WT cells, in both MDA-MB-231 and HeLa cells (Fig. 2C). Immunofluorescence staining clearly showed that p-FAK containing cell matrix adhesion in S3-5 cells was consistently more prominent in both size and staining intensity than that in WT-MDA-MB-231 cells (Fig. 2D, top). Furthermore, the actin stress fibers detected by phalloidin were more abundant in S3-5-HeLa cells than in WT cells (Fig. 2D, bottom). Considering the decreased cell migration ability of S3-5 cells, these findings indicate that integrin α5 *N*-glycosylation can regulate a modest level of cell-FN adhesion for migration.

Removal of *N*-glycosylation on integrin α5 increases the active form of β1 on the cell surface. Next, we investigated the cause of increased cell-FN adhesion in S3-5 cells. Considering that the efficiency of cell adhesion on the ECM is generally thought to be proportional to the amount of either active or total (i.e., active and inactive) integrin on the cell surface (17), we compared the expression levels of both active and total integrin β1 in WT and S3-5 cells. The active form of β1 was detected with the antibody HUTS-4-recognizing epitopes in the region spanning positions 355 to 425 (hybrid domain) of the common β1 subunit, the expressions of which are reported to parallel the activity of integrin β1 (18), and the level of active integrin β1 recognized by this antibody but not total β1 was clearly increased upon Mn^{2+} stimulation during Western blot analysis (see Fig. S1F in the supplemental material). Flow cytometric analysis clearly showed that approximately 10% of cell surface integrin β1 is in the active conformation (Fig. 3A), which is consistent with data from a previous report (19), and that levels of the active form of β1 but not the total form on the cell surface were significantly increased in S3-5-MDA-MB-231, S3-5-HeLa, and S3-5-U-251MG cells compared with those in WT cells (Fig. 3A).

Given the increased expression levels of active β1 on the cell surface of S3-5 mutant cells, we wondered whether the expression of total active β1 was also increased. Interestingly, as shown in Fig. 3B (middle), both WT and S3-5 mutant cells exhibited expression levels of both active β1 and total β1 similar to those in the whole-cell lysates. However, increased expression levels of active β1 on the cell surface in S3-5 cells, as described above, were observed in the biotinylation experiment (Fig. 3B, top). Furthermore, the increased cell surface expression of active integrin β1 (Fig. 3C, middle), but not that of the total version (Fig. 3C, top), in mutant MDA-MB-231 cells was consistently confirmed by immunostaining. Taken together, these results indicate that the *N*-glycosylation of α5 can regulate the localization of the active form of β1 on the cell surface, which might explain the enhancement of cell-FN adhesion in S3-5 mutant cells.

***N*-Glycosylation on integrin α5 plays important roles in the internalization of active $\alpha5\beta1$.** Because the loss of *N*-glycosylation on α5 increased the expression levels of active β1 on the cell surface, we sought to investigate the underlying mechanism. Given that the endocytic trafficking of integrins, which involves their internalization from the cell surface and recycling back to the plasma membrane, is important for cell migration (20) and expression levels on the cell surface (21), we wondered whether *N*-glycosylation on α5 regulates its internalization. To address this, biotin pulse-chase experiments were performed. After biotin labeling of cell surface proteins at 4°C, cells were incubated at 37°C for different times to induce internalization, and the biotin remaining in the form of cell surface proteins was then stripped at 4°C, leaving only

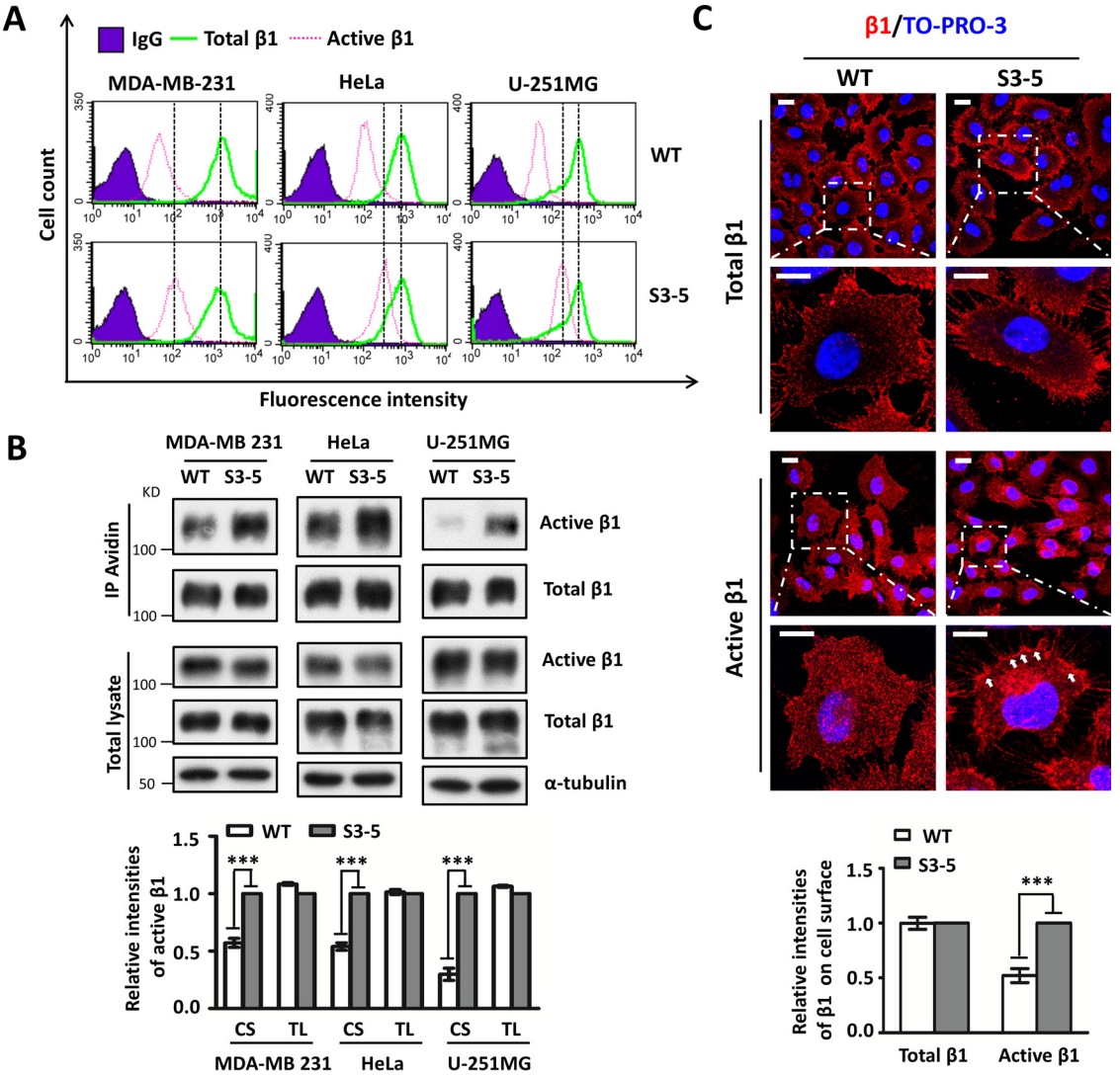

FIG 3 Increased expression levels of active integrin $\beta 1$ in S3-5 mutant cells. (A and B) The expression levels of active and total integrin $\beta 1$ on the cell surface (CS) or in total cell lysates (TL) were analyzed by flow cytometry (A) or biotinylation (B), and immunoblotting was performed with the indicated antibodies. The relative ratio (active $\beta 1$ versus total $\beta 1$) is shown at the bottom ($n = 3$ individual experiments), which was 1.0 for S3-5 mutant cells. (C) Comparison of the localization patterns of active integrin $\beta 1$ in WT- and S3-5-MDA-MB-231 cells. Cells were cultured on FN-coated coverslips and then subjected to immunostaining analyses. The images were merged with total (top) or active (middle) integrin $\beta 1$ (red) and To-Pro-3 staining (blue). The relative fluorescence intensities of total $\beta 1$ and active $\beta 1$ on cell surface were quantified by using ImageJ software ($n = 6$, from 3 individual experiments); relative fluorescence intensity was 1.0 for S3-5 mutant cells (bottom). All values are reported as the means ± SE (error bars), as determined by Student's *t* test. ***, $P < 0.001$. Bars, 20 μm (C).

internalized proteins biotinylated. Internalization of integrin $\alpha 5\beta 1$ was quantified by the immunoprecipitation of streptavidin-agarose, followed by Western blot analysis. As shown in Fig. 4A and B, the internalization of active $\beta 1$ in WT cells was increased within 5 min and then decreased at 10 min, while it continued to increase even at 15 min in S3-5 mutant cells, indicating delayed internalization in mutant cells. However, there were no significant differences in the internalizations of total $\alpha 5$ or $\beta 1$ subunits between WT and mutant cells. Consistently, the delayed internalization of active $\beta 1$ in S3-5 mutant cells was also confirmed by a biotinylation-based capture enzyme-linked immunosorbent assay (ELISA) (Fig. 4C). Taken together, these data indicate that *N*-glycosylation serves as a switch to control the internalization of active, but not inactive, integrin $\alpha 5\beta 1$.

Site 1 and site 2 *N*-glycosylation of the β-propeller domain on $\alpha 5$ mediates the regulation of cell migration. The data described above led us to investigate which

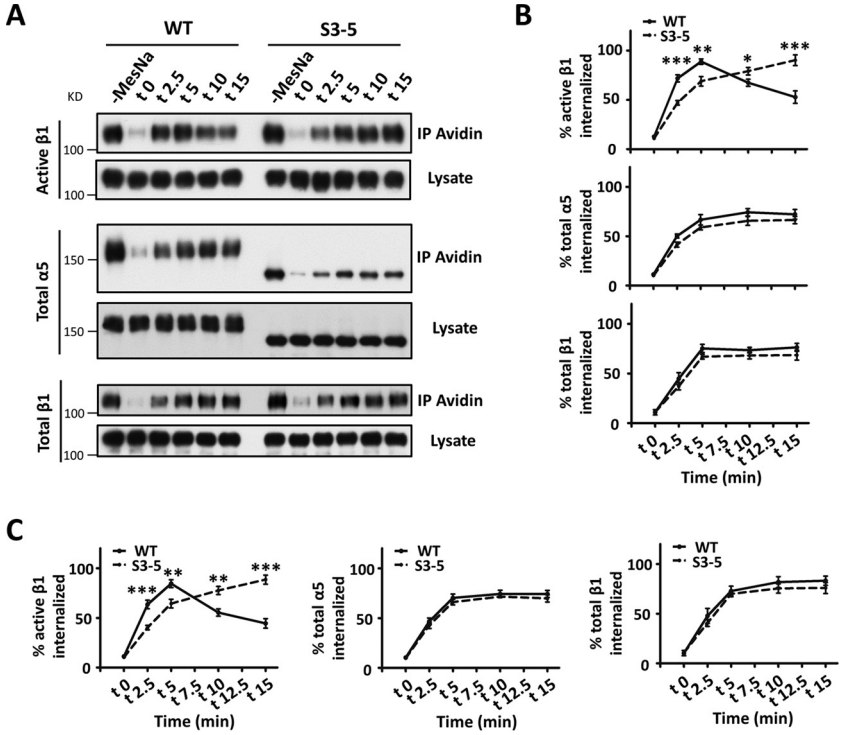

FIG 4 Delayed internalization of active integrin β1 in S3-5 mutant MDA-MB-231 cells. (A) A biochemical internalization assay of active integrin β1, total integrin α5, and total integrin β1 was performed. The indicated internalized integrins at the indicated times were immunoprecipitated by avidin-agarose and then subjected to Western blotting for detection. The cell lysates were used as controls to show similar expression levels of the indicated integrins between WT and S3-5 cells. (B) The percentages of internalized integrins were statistically calculated from the signal intensity of MesNa-resistant integrin at each time point relative to the value for the control groups (without MesNa), which was the total integrin on the cell surface ($n = 3$ individual experiments). (C) The proportions of internalized integrins of WT and S3-5 mutant cells during the internalization period were also determined by a capture ELISA using microtiter wells coated with anti-active integrin β1, anti-integrin α5, or anti-integrin β1 antibodies, as described in Materials and Methods. The proportions of internalized integrins were statistically calculated ($n = 3$ individual experiments). All values are reported as the means $\pm$ SE (error bars), as determined by Student's *t* test. *, $P < 0.05$; **, $P < 0.01$; ***, $P < 0.001$.

N-glycosylation site(s) of integrin α5 was essential for regulation. We recently demonstrated that *N*-glycosylation of the calf domain on α5 (sites 10 to 14) (Fig. 5A) was essential for its association with EGFR (15). This represented the first restoration of *N*-glycosylation in both the calf and the remaining domains in S3-5 mutant cells. However, as shown in Fig. 5B and C, restoration of *N*-glycosylation on the calf domain (sites 3 to 5 and 10 to 14) affected neither cell migration nor the expression of active β1 on the cell surface. Furthermore, deletion of the *N*-glycosylation sites on the calf domain (sites 1 to 9) enhanced cell migration (Fig. 5B) and decreased the expression level of active β1 on the cell surface (Fig. 5C), which was similar to the reaction in WT cells and highlighted the importance of *N*-glycosylation on the β-propeller and thigh domains (sites 1 to 9) of integrin α5. Furthermore, the restoration of *N*-glycosylation on the β-propeller domain (sites 1 to 5), but not that on the thigh domain (sites 3 to 9), largely rescued the cell migration ability (Fig. 5B). Consistently, the increased expression levels of active β1 on the cell surface of S3-5 cells was almost normalized in S1-5 mutant cells compared with that in WT or S1-9 mutant cells (Fig. 5C). Moreover, importantly, the delayed internalization of active β1 (Fig. 5D) and the enhanced expression levels of p-FAK in S3-5 cells were also reversed in S1-5 but not S3-9 cells (Fig. 5E), indicating that site 1 and site 2 *N*-glycosylation on α5 was most important for active β1-mediated appropriate cell adhesion for migration. Of note, as shown in Fig. S1B in the supplemental material, all the mutant cells exhibited almost the same expression levels of integrin α5 on the cell surface compared with the WT ones, further suggesting that the

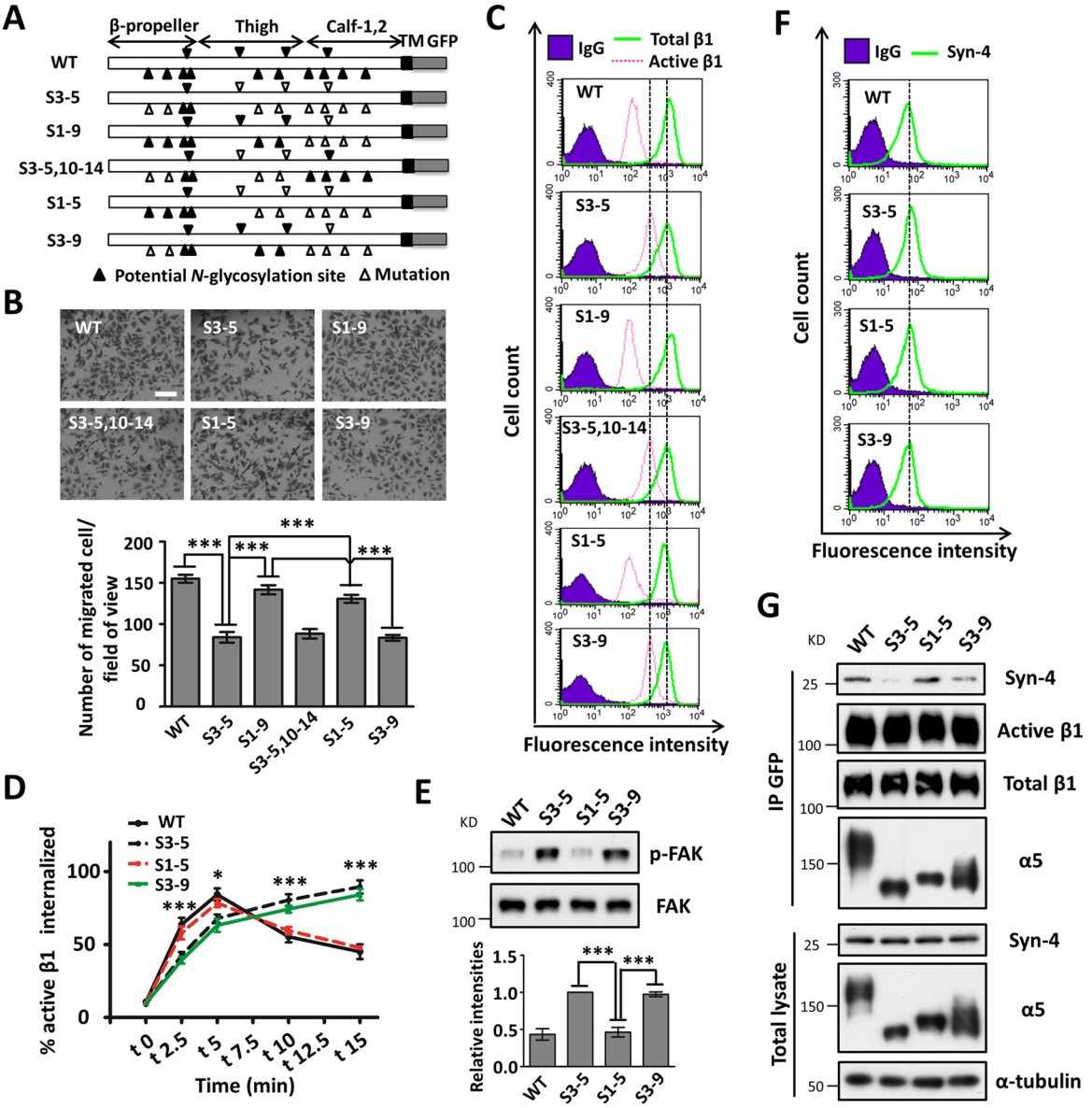

FIG 5 Importance of *N*-glycosylation on the β-propeller domain of α5 for cell migration and α5–syndecan-4 complex formation. (A) Schematic diagram of potential *N*-glycosylation sites on the WT and mutational α5 subunits (S3-5; S1-9; S3-5,10-14; S1-5; and S3-9). (B) Comparison of the cell migration abilities among WT and mutant cells with restored S1-9; S3-5,10-14; S1-5; or S3-9 α5. The stable cell lines were established as described in Materials and Methods. The cell migration abilities were analyzed ($n = 3$ individual experiments). (C) The expression levels of active and total β1 were analyzed by flow cytometry. (D) The internalization of active integrin β1 in WT, S3-5, S1-5, and S3-9 mutant cells was determined by a capture ELISA. The proportions of internalized active β1 were statistically calculated ($n = 3$ individual experiments). (E, top) After culture on FN-coated dishes for 2 days, the indicated MDA-MB-231 cells were lysed and immunoblotted with the indicated antibodies. (Bottom) Relative ratios (p-FAK versus FAK) ($n = 3$ individual experiments); the relative ratio was 1.0 for S3-5 mutant cells. (F) The surface expression levels of syndecan-4 on WT and S3-5, S1-5, and S3-9 mutant cells were analyzed by flow cytometry. (G, top) The indicated MDA-MB-231 cell extracts were immunoprecipitated with anti-GFP–agarose followed by anti-syndecan-4 (Syn-4), active β1, total β1, and α5 antibodies for Western blotting. (Bottom) Whole-cell extracts were also immunoblotted with the indicated antibodies. All values are reported as the means ± SE (error bars), as determined by Student's *t* test; *, $P < 0.05$; ***, $P < 0.001$. Bar, 350 μm (B).

remaining *N*-glycosylation sites, with the noted exception of sites 3 to 5 of integrin α5, had no effect on its expression.

Next, we explored the underlying mechanisms of the *N*-glycosylation of integrin α5-mediated activation and migration. Considering that integrin-mediated cellular events are thought to be regulated not only by a conformational change caused by their activations but also by their cross talk with other membrane proteins (22), we further investigated $\alpha5\beta1$-mediated complex formation. Here, we chose one representative membrane protein, syndecan-4, a transmembrane heparan sulfate proteoglycan

that can interact with integrin α5β1 (23) and has been reported to be a control protein for α5β1 trafficking (24). As shown in Fig. 5F, WT and S3-5, S1-5, and S3-9 mutant cells exhibited same expression levels of syndecan-4 on the cell surface as determined by flow cytometry, suggesting that *N*-glycosylation on α5 had no effect on the expression of syndecan-4. However, immunoprecipitates with anti-GFP–agarose showed that the interaction between syndecan-4 and α5 was significantly decreased in S3-5 cells (Fig. 5G). Importantly, the decreased association between α5 and syndecan-4 could be reversed in S1-5 but not S3-9 cells (Fig. 5G), which indicated that site 1 and site 2 *N*-glycosylation on α5 was required for its cooperation with syndecan-4. In addition, these four cell lines exhibited almost the same association abilities between α5 and active or total β1 (Fig. 5G), which further suggested that *N*-glycosylation on α5 had no significant effect on the heterodimerization of α5β1. It is notable that the expression levels of active β1 on the cell surface were significantly different among these mutants (Fig. 5C), but the total expression levels of active β1 were almost the same, as shown in Fig. 3B and 5G. In fact, based on data from previous reports, the active β1 integrins were predominantly cytoplasmic (19, 25), as also shown in Fig. 3C. Taken together, these results clearly showed that site 1 and site 2 *N*-glycosylation on the β-propeller domain of α5 plays a crucial role in regulating appropriate cell adhesion for migration by controlling the internalization of its active form and complex formation (e.g., syndecan-4), which demonstrates a novel mechanism for integrin α5-mediated cell migration.

DISCUSSION

Previously, our group identified specific *N*-glycosylation on integrin α5 that plays crucial roles in several biological functions. In detail, we first underscored the importance of three *N*-glycosylation sites (sites 3 to 5 and particularly site 5) on the β-propeller domain of α5 in its heterodimeric formation with β1 (12). Also, we recently identified that *N*-glycosylation on the calf domain, at sites 10 to 14, was essential for the α5-mediated inhibitory effect on EGFR signaling and cell proliferation (15). Here, we expanded our understanding of the *N*-glycosylation of α5 and found that site 1 and site 2 *N*-glycosylation on the β-propeller domain plays a key role in driving integrin α5β1 dynamics and cell migration, which is a central role for integrin. Mechanistically, site 1 and site 2 *N*-glycosylation regulates complex formation with syndecan-4, which probably enhances active integrin α5β1 internalization and promotes FA disassembly to provide modest cell-substrate adhesiveness for cell migration (Fig. 6). Taken together, these findings support the idea that individual integrin α5 *N*-glycosylation differentially functions as a molecular switch to regulate the biological functions of α5β1.

The *N*-glycosylation of α5 is widely believed to play important roles in cell migration through several experimental methods, including the remodeling of *N*-glycans by treatment with *N*-glycanase F or an *N*-linked oligosaccharide-processing inhibitor and manipulation of the expression levels of some important glycosyltransferases (14). Apparently, the use of these models to comprehensively explore the functions of α5 *N*-glycosylation and its underlying mechanisms is insufficient, because those studies lacked strict control. In the present study, we clearly demonstrated that the removal of the majority of α5 *N*-glycosylation, except for that on sites 3 to 5, affected neither α5β1 heterodimer formation nor cell surface expression or cell spreading, but it dramatically suppressed cell migration in several cancer cell lines, including MDA-MB-231, HeLa, and U-251MG cells. These data suggest that α5 *N*-glycosylation, with the exception of sites 3 to 5, is important for cell migration. These results seem contradictory compared to those of our previous study, in which CHO-B2-S3-5 mutant cells exhibited cell spreading and migration abilities on FN comparable to those of the WT (12). These differences could be explained at least in part by the lack of α2,6-sialylation expression in the CHO-B2 cell line (26), since α2,6-sialylation plays very important roles in integrin α5β1-mediated cell migration and other functions (27).

FAK is a key molecule in integrin-mediated cell adhesion and migration, and the autophosphorylation of FAK at tyrosine 397 plays important roles not only in intracellular signaling but also in cell motility (28). Unexpectedly, the phosphorylated levels of

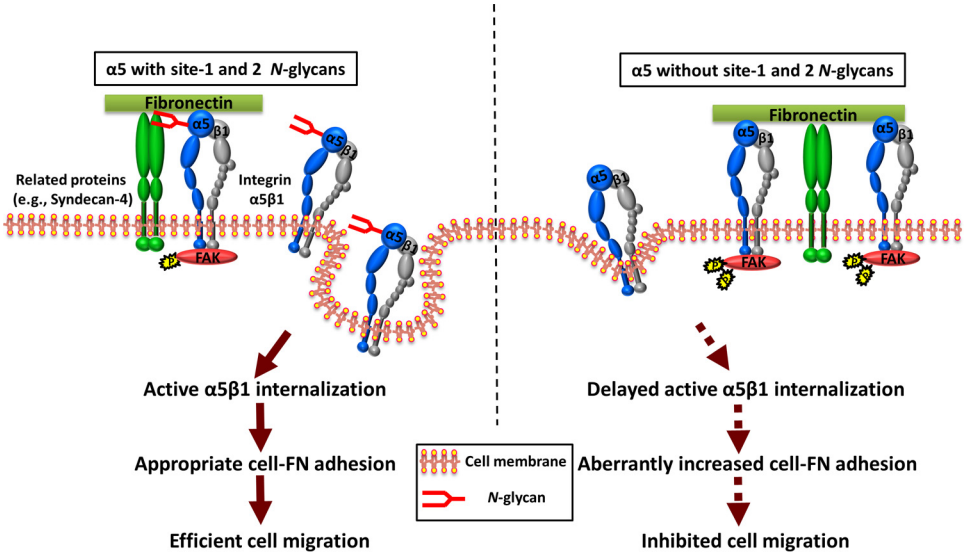

FIG 6 Proposed model for the regulation of integrin $\alpha5\beta1$-mediated cell migration by *N*-glycosylation. (Left) Integrin $\alpha5\beta1$ may form a complex with several receptors (e.g., syndecan-4), which may trigger active $\alpha5\beta1$ internalization and the turnover of FA to provide the appropriate cell-substrate adhesiveness for efficient cell migration. (Right) However, in the case of the $\alpha5$ mutant lacking *N*-glycosylation on sites 1 and 2, the cells exhibit increased active $\alpha5\beta1$ expression on the cell surface and enhanced cell adhesion signaling as a result of its decreased ability to associate with related proteins, which results in the suppression of cell migration. The present study provides new insights into the concept that modest cell adhesion is best for cell migration (40). The solid arrows indicate a normal signal pathway in integrin $\alpha5\beta1$-mediated cell migration, while the dotted arrows indicate that these events are aberrant.

FAK upon FN stimulation in S3-5 mutant cells were higher than those in WT cells. Furthermore, actin stress fiber formation was also greatly enhanced in the mutant cells. These data further support the notion that more cell-substrate adhesiveness, less cell migration, and a modest amount of cell adhesion are important for cell migration (29). In fact, cell migration is a strictly controlled dynamic process, which requires regulated cycles of polarized cell-substrate attachment to form focal contact at the leading edge of the cell with corresponding detachment at its trailing edge (30). Therefore, an imbalance of attachment and detachment in this process may result in abnormal adhesion (31). Such a cell adhesion phenotype is compatible with data from a previous study in which a loss of the protein annexin A2 inhibited intestinal epithelial cell migration while promoting enhanced cell matrix adhesion (21). Given that the conformational activation of integrins on the cell surface supports cell adhesion and spreading, whereas the transition of integrins toward an inactive bent conformation causes cell detachment and rounding (32, 33), it is possible that the increased cell adhesion ability is due to an aberrant activation of integrin. In agreement with this hypothesis, our flow cytometric and biotinylation analyses showed that S3-5 mutant cells highly expressed the active form of $\alpha5\beta1$ on the cell surface. Similarly, Park et al. previously reported that aberrant activation of integrin $\alpha4\beta7$ suppressed lymphocyte migration and underscored the importance of a proper balance in the adhesion and de-adhesion of integrin (34). The enhanced expression of active $\beta1$ on the cell surface might have been due to different trafficking events, since the internalization of the active form of $\alpha5\beta1$ but not the total version was significantly delayed in S3-5 cells compared with that in WT cells. These results suggested that $\alpha5$ *N*-glycosylation may have a significant effect on the expression and internalization of active $\alpha5\beta1$. Our finding is analogous to those of a previous report indicating that the downregulation of the protein neuropilin-1 (Nrp1) resulted in a delay in active integrin $\alpha5\beta1$ internalization but not that of the total version (35). Therefore, it is reasonable to consider that the internalization of active and inactive integrins may occur through distinct molecular mechanisms. Actually, inactive and active integrins $\alpha5\beta1$ undergo different trafficking path-

ways: the Rab4-dependent short loop for inactive integrin β1 (19) and the Rab11-dependent long loop used by active $\alpha5\beta1$ (20). Thus, further studies elucidating the functions of α5 *N*-glycosylation in regulating its degradation and recycling are required for a comprehensive understanding of how *N*-glycosylation coordinates the trafficking of integrin $\alpha5\beta1$ during cell migration.

Integrin $\alpha5\beta1$ internalization is the first step in its trafficking. It is required for the disassembly regulation of FA and plays a key role in efficient cell migration (34). However, the current mechanism for integrin $\alpha5\beta1$ internalization remains largely unclear, since most studies focus mainly on intracellular trafficking regulation without extracellular information (7, 9). Here, we found the site 1 and site 2 *N*-glycosylation on α5 could regulate active $\alpha5\beta1$ internalization, which may broaden our understanding of the functions of the extracellular domains in $\alpha5\beta1$ trafficking. In addition, the internalization of $\alpha5\beta1$ is also related to the assistance of other transmembrane proteins such as the FN receptor syndecan-4 (24, 36), myelin-associated glycoprotein (37), EGFR (38), and Nrp1 (35). As a model, here we focused on syndecan-4 and found that its associative ability with $\alpha5\beta1$ was dependent on α5 *N*-glycosylation. In particular, site 1 and site 2 *N*-glycosylation of α5 was most important for interactions and cell migration. Of course, we could not exclude the effects of cell migration on the remaining *N*-glycosylation sites. In fact, the restoration of site 1 and site 2 *N*-glycosylation in the S3-5 mutant efficiently rescued the expression of the active form of β1 to a level similar to that in WT cells, whereas the cell migration ability was only partially rescued. This is a possible reason why *N*-glycosylation on the calf domain (sites 10 to 14) of α5 is necessary for EGFR-α5 complex formation, as previously reported (15), which may also play important roles in $\alpha5\beta1$ trafficking and cell migration, as discussed above. Moreover, it is of note that the internalization ratio of active β1 in S3-9 cells was slightly higher than that in S3-5 cells to some extent but was not significant (Fig. 5E), and also, there was a weak interaction between α5 and syndecan-4 in S3-9 mutant cells (Fig. 5G), which may indicate that *N*-glycosylation on the thigh domain of α5 also has some effects on the internalization of active β1. Considering the roles of the bulky glycocalyx of the ECM in integrin-mediated tumor phenotypes (39), it is tempting to speculate that individual *N*-glycosylation on integrin may exhibit a suitable physical or specific structure that functions as a nexus for integrin-mediated complex formation to integrate both the ECM and cytokines in the microenvironment surrounding tumors.

In summary, we have delineated the mechanism for *N*-glycosylation on the β-propeller domain of α5 as a controller that coordinates cell-FN adhesion and internalization dynamics of $\alpha5\beta1$ for cell migration. These findings will improve our understanding of how cell-substrate adhesiveness is regulated and the importance of a modest level of cell adhesion for cell migration.

MATERIALS AND METHODS

Antibodies and reagents. The experiments were performed by using the following antibodies: monoclonal antibodies (MAbs) against integrin α5, integrin β1, integrin α6, p-FAK, and FAK (BD Biosciences, San Jose, CA); MAbs against human $\alpha5\beta1$ (HA5), active integrin β1 (HUTS-4), integrin α3, and integrin β4 and rabbit polyclonal antibody against integrin α5 (Millipore, Billerica, MA); mouse MAb to syndecan-4 (Santa Cruz Biotechnology, Santa Cruz, CA); antibody against integrin αV (BioLegend, San Diego, CA); MAb against the human integrin β1 subunit (P5D2) (Developmental Studies Hybridoma Bank, University of Iowa, IA); MAb against α-tubulin (Sigma-Aldrich, St. Louis, MO); and Alexa Fluor 647– or 546–goat anti-mouse IgG and Alexa Fluor 546-phalloidin (Thermo Fisher Scientific, Waltham, MA). The peroxidase-conjugated goat antibodies against mouse and rabbit IgG were obtained from Chemicon and Cell Signaling Technology (Danvers, MA), respectively. 2-Mercaptoethanesulfonic acid sodium salt (MesNa), iodoacetamide, *o*-Phenylenediamine dihydrochloride (OPD), and FN were obtained from Sigma; control mouse IgG1 was obtained from Tonbo Biosciences (San Diego, CA); and sulfo-NHS-SS biotin (sulfosuccinimidyl-2-[biotinamido]ethyl-1,3-dithiopropionate), streptavidin-conjugated horseradish peroxidase, and To-Pro-3 were obtained from Thermo Fisher Scientific. PNGase F, agarose-conjugated anti-GFP antibody (RQ2), streptavidin-conjugated agarose, and Ab-Capture Extra beads were obtained from New England BioLabs, Medical & Biological Laboratories Co. Ltd. (Nagoya, Japan), Millipore, and ProteNova Co. Ltd. (Kagawa, Japan), respectively.

Cell lines and cell culture. The 293T and HeLa cell lines were provided by the RIKEN cell bank (Tokyo, Japan). The MDA-MB-231 cell lines were purchased from the American Type Culture Collection (Manassas, VA). The U-251MG cell line was a gift from Jun Nakayama (Shinshu University Graduate School

of Medicine, Japan). Integrin α5-KO-MDA-MB-231, α5-KO-HeLa, and α5-KO-U-251MG cells were previously established in our laboratory (15). The stable cell lines used in this study were established as mentioned below. All cell lines were maintained at 37°C in Dulbecco's modified Eagle's medium (DMEM) supplemented with 10% fetal bovine serum (FBS) under a humidified atmosphere containing 5% CO_2, except for virus production.

Integrin α5 expression vectors. The pENTR-D-Topo vectors of GFP and GFP-tagged integrin α5 with altered *N*-glycosylation sites (the WT and the S3-5; S1-9; S3-5,10-14; and S1-5 mutants) were previously established in our laboratory (12, 15). The mutation vector S3-9 was constructed by using an in-fusion kit (TaKaRa Bio) according to the manufacturer's instructions and then cloned into the CSII-EF-Rfa vector by using a Gateway cloning system kit (Thermo Fisher Scientific) to acquire all lentivirus expression vectors.

Virus production, infection, and stable cell line construction. Virus production and infection were performed as described previously (15). In brief, CSII-EF-Rfa-based lentivirus vectors were cotransfected with pCAG-HIVgp and pCMV-VSV-G-RSV-Rev into 293T cells. After transfection for 48 h, the lentivirus supernatants were collected. The indicated integrin α5 KO cells were infected with the resultant viral supernatant for 72 h, and GFP-positive cells were then sorted 3 times by using a FACSAria II instrument. Stable cell lines were used in subsequent studies.

Cell spreading and cell adhesion response assays. Six-well plates were coated with FN (10 μg/ml) in phosphate-buffered saline (PBS) overnight at 4°C and then blocked with 1% bovine serum albumin (BSA) in DMEM for 1 h at 37°C. The indicated cells were detached and suspended in assay medium (50 mM HEPES and 0.1% BSA in serum-free DMEM [pH 7.4]) for 40 min at 3×10^4 cells/ml. After a 20-min incubation, nonadherent cells were gently removed by washing with PBS, attached cells were fixed with 4% paraformaldehyde (PFA) in PBS, and photos were then taken by phase-contrast microscopy.

To assay the cell adhesion response upon FN treatment, the indicated cells were also detached and suspended in the assay medium for 40 min at 1×10^6 cells/ml. After replating onto FN-coated 6-well plates for 0, 15, 30, and 45 min, nonadherent cells were gently removed by washing with PBS, and the attached cells were collected, lysed, and then analyzed by WB, as described below.

Video microscope. A glass-bottom dish (Asahi Techno Glass, Japan) was precoated with 10 μg/ml FN at 4°C overnight and then blocked with 1% BSA in DMEM for 1 h at 37°C. A 2-ml aliquot of the cell suspension (2.5×10^4 cells/ml) in serum-free DMEM was added to each glass-bottom dish. After incubation for 1 h to allow cells to adhere to FN, the serum-free medium was gently replaced with 2 ml growth medium, followed by mounting with 1 ml glycerol. The cells were then monitored, and the images and videos were acquired by using inverted microscopes (Axio Observer.D1; Carl Zeiss) every 10 min at 37°C with 5% CO_2 in a heated chamber with temperature and CO_2 control (Onpu-4 & CO_2; Air Brown, Japan). Cell motility was analyzed in roughly 12 cells by measuring the *x* and *y* coordinates of tracked cells over 12 h. The directionality (ratio of the Euclidean distance versus accumulated distance, $0 \leq$ values ≤ 1) parameters, displacement (micrometers), and the manual tracking plug-in velocity (micrometers per minute) were analyzed by using Chemotaxis and Migration Tool software (version 2.0).

Wound healing assay. A confluent layer of cells cultured on an FN-coated (10 μg/ml) 6-well plate was starved in serum-free medium for 12 h and then scraped by using a p200 pipette tip. Serum-free medium was replaced with 3% FBS-containing DMEM. Wounded areas were photographed under a light microscope at 0 and 24 h for MDA-MB-231 cells, at 36 h for HeLa cells, and at 48 h for U-251MG cells. Wound closure was measured by observing the distances between the sides of the wound at the indicated times.

Cell migration assay. Each Transwell (BD BioCoat control 8.0-μm-pore-size inserts) was coated only on the bottom side with 10 μg/ml FN at 4°C overnight. Cells were prestarved in serum-free medium for 12 h, trypsinized, and suspended in complete DMEM. The suspended cells were centrifuged, and the supernatants were removed. The resultant cell pellets were resuspended with assay medium (0.1% BSA in DMEM containing 3% FBS) and diluted to 1×10^5 cells/ml, and the cell viabilities were confirmed by trypan blue staining. Aliquots of 500 μl of the cell suspension were added to each FN-coated Transwell, followed by incubation at 37°C for 5 h for HeLa cells and for 4 h for MDA-MB-231 or U-251MG cells. After incubation, cells on the upper side were gently removed by scraping with a cotton swab. The membranes in the Transwells were fixed with 4% PFA for 30 min, followed by staining with 0.5% crystal violet for 4 h. Cells that had migrated to the lower side were counted by using a phase-contrast microscope.

Western blot and immunoprecipitation analyses. For WB, the indicated cells were washed with ice-cold PBS and then lysed in the cell lysate (20 mM Tris-HCl [pH 7.4], 150 mM NaCl, 1% Triton X-100) with protease and phosphatase inhibitors (Nacalai Tesque, Kyoto, Japan) for 30 min. After centrifugation, the supernatant was collected, and protein concentrations were determined by using a bicinchoninic acid (BCA) protein assay kit (Pierce, Rockford, IL). The protein samples were resolved by nonreducing SDS-PAGE for α5 and active β1 or reducing SDS-PAGE for other proteins. After electrophoresis, the proteins were transferred onto a polyvinylidene difluoride (PVDF) membrane (Millipore) and detected with the indicated primary and secondary antibodies by using the Immobilon Western chemiluminescent horseradish peroxidase (HRP) substrate (Millipore), according to the manufacturer's instructions. For IP, cells were lysed in 0.1% Triton–Tris-buffered saline (TBS) buffer (20 mM Tris-HCl [pH 7.4], 150 mM NaCl) with a protease inhibitor and then centrifuged. The supernatants were immunoprecipitated with anti-GFP–agarose for 1 h at 4°C with rotation, and the immunoprecipitates were subjected to SDS-PAGE.

PNGase F treatment. The indicated cell lysates were treated with PNGase F at 37°C for 1 h according to the manufacturer's instructions or not treated and then subjected to SDS-PAGE with the indicated antibodies.

Flow cytometric analysis. The indicated semiconfluent cells were detached from 10-cm culture dishes and subsequently stained with either mouse IgG or primary antibodies for 1 h on ice, followed by

incubation with Alexa Fluor 647–goat anti-mouse IgG for 1 h. During incubation, the cells were mixed gently every 10 min by flicking. After incubation, cells were washed and then analyzed by using a FACSCalibur flow cytometer (BD Biosciences).

Cell surface biotinylation. Cells were gently washed twice with PBS and then incubated with ice-cold PBS containing 0.2 mg/ml sulfo-NHS-SS biotin for 1 h at 4°C. After incubation, cells were washed 3 times with ice-cold PBS, and the cells were harvested by using lysis buffer. A total of 200 μg of the biotinylated protein was precipitated with streptavidin-conjugated agarose (20 μl) for another 1 h at 4°C with rotation and then subjected to SDS-PAGE as described above.

Immunofluorescence. Cells were plated onto FN-coated glass coverslips (MatTek Corporation, Ashland, MA) for 48 h, washed with PBS, fixed with 4% PFA, and blocked with PBS–0.1% Triton X-100–10% BSA. Antibodies against p-FAK, active β1, or P5D2 were used, followed by incubation with anti-mouse Alexa Fluor 546-conjugated secondary antibodies and Alexa Fluor 546-phalloidin. Finally, the cells were incubated with To-Pro-3 for 30 min. The confocal images were also acquired by using a 60×/1.35-numerical-aperture (NA) oil immersion objective lens (FV1000; Olympus, Tokyo, Japan). The fluorescence intensities were quantified by using ImageJ software.

Capture ELISA. Corning (Corning, NY) 96-well enzyme immunoassay (EIA)/radioimmunoassay (RIA) plates were coated with 5 μg/ml the appropriate anti-integrin antibodies in 0.05 M Na_2CO_3 (pH 9.6) at 4°C overnight and then blocked in PBS containing 0.05% Tween 20 (PBS-T) with 5% BSA for 1 h at room temperature. The indicated integrins were captured by incubation of 50 μl (about 80 μg) of the cell lysate overnight at 4°C. Unbound material was removed by extensive washing with PBS-T, and wells were incubated with streptavidin-conjugated horseradish peroxidase in PBS-T containing 1% BSA for 1 h at 4°C. Following further washing, biotinylated integrins were detected by a chromogenic reaction with OPD for 20 min, and the absorbances at 450 nm were measured.

Biotinylation-based integrin internalization assay. Cells grown on FN-coated 10-cm dishes were serum starved for 1 h prior to the assay and washed with ice-cold PBS, and surface proteins were biotinylated with 0.2 mg/ml sulfo-NHS-SS biotin in PBS for 1 h, followed by washing in TBS and placement in a cold room. For internalization, cells were then incubated in prewarmed complete DMEM at 37°C for 0, 2.5, 5, 10, and 15 min, whereas the control groups (without MesNa) remained on ice. Surface biotin was then stripped from the cells with 10 min of incubation in 50 mM MesNa–TBS (pH 8.6) twice, followed by washing and quenching of MesNa with 20 mM iodoacetamide in TBS for 10 min. Cells of the control group were not subjected to surface reduction (without MesNa) in order to obtain total surface-labeled integrin. After quenching, the cells were lysed, precipitated with streptavidin-conjugated agarose, and subjected to WB or a capture ELISA.

Statistical analysis. Results are reported as the means ± standard errors (SE). Statistical analyses were performed by using Student's *t* test and GraphPad Prism version 5. Statistical significance was defined as a *P* value of <0.05.

SUPPLEMENTAL MATERIAL

Supplemental material for this article may be found at https://doi.org/10.1128/MCB.00558-16.

SUPPLEMENTAL FILE 1, PDF file, 0.8 MB.

ACKNOWLEDGMENTS

Q.H. performed all the experiments with the help of T.I., S.H., Y.W., and T.F. Q.H. and T.I. constructed the virus expression and the α5 knockout vectors. Q.H., T.F., and S.H. did the cell sorting experiments and constructed the related stable cell lines. J.G. designed the experiment. Q.H. and J.G. analyzed the data, prepared the figures, and wrote the manuscript. All authors discussed the results and commented on the manuscript.

We declare no competing financial interests.

This work was partially supported by grants-in-aid for scientific research (15H04354 to J.G. and 24570169 to T.I.) and for Challenging Exploratory Research (15K14408 to J.G.) from the Japan Society for the Promotion of Science, a grant from the National Natural Science Foundation of China (no. 31670807), and a Strategic Research Foundation grant-aided project for private universities from the Ministry of Education, Culture, Sports, Science, and Technology of Japan.

REFERENCES

1. Franz CM, Jones GE, Ridley AJ. 2002. Cell migration in development and disease. Dev Cell 2:153–158. https://doi.org/10.1016/S1534-5807(02)00120-X.
2. Hynes RO. 2002. Integrins: bidirectional, allosteric signaling machines. Cell 110:673–687. https://doi.org/10.1016/S0092-8674(02)00971-6.
3. Wolfenson H, Lavelin I, Geiger B. 2013. Dynamic regulation of the structure and functions of integrin adhesions. Dev Cell 24:447–458. https://doi.org/10.1016/j.devcel.2013.02.012.
4. Kim C, Ye F, Ginsberg MH. 2011. Regulation of integrin activation. Annu Rev Cell Dev Biol 27:321–345. https://doi.org/10.1146/annurev-cellbio-100109-104104.
5. Shattil SJ, Kim C, Ginsberg MH. 2010. The final steps of integrin activation:

the end game. Nat Rev Mol Cell Biol 11:288–300. https://doi.org/10.1038/nrm2871.
6. Margadant C, Monsuur HN, Norman JC, Sonnenberg A. 2011. Mechanisms of integrin activation and trafficking. Curr Opin Cell Biol 23:607–614. https://doi.org/10.1016/j.ceb.2011.08.005.
7. Caswell PT, Vadrevu S, Norman JC. 2009. Integrins: masters and slaves of endocytic transport. Nat Rev Mol Cell Biol 10:843–853. https://doi.org/10.1038/nrm2799.
8. Margadant C, Kreft M, de Groot DJ, Norman JC, Sonnenberg A. 2012. Distinct roles of talin and kindlin in regulating integrin alpha5beta1 function and trafficking. Curr Biol 22:1554–1563. https://doi.org/10.1016/j.cub.2012.06.060.
9. Bridgewater RE, Norman JC, Caswell PT. 2012. Integrin trafficking at a glance. J Cell Sci 125:3695–3701. https://doi.org/10.1242/jcs.095810.
10. Gu J, Taniguchi N. 2004. Regulation of integrin functions by N-glycans. Glycoconj J 21:9–15. https://doi.org/10.1023/B:GLYC.0000043741.47559.30.
11. Isaji T, Sato Y, Fukuda T, Gu J. 2009. N-Glycosylation of the I-like domain of beta1 integrin is essential for beta1 integrin expression and biological function: identification of the minimal N-glycosylation requirement for alpha5beta1. J Biol Chem 284:12207–12216. https://doi.org/10.1074/jbc.M807920200.
12. Isaji T, Sato Y, Zhao Y, Miyoshi E, Wada Y, Taniguchi N, Gu J. 2006. N-Glycosylation of the beta-propeller domain of the integrin alpha5 subunit is essential for alpha5beta1 heterodimerization, expression on the cell surface, and its biological function. J Biol Chem 281:33258–33267. https://doi.org/10.1074/jbc.M607771200.
13. Takahashi M, Kizuka Y, Ohtsubo K, Gu J, Taniguchi N. 27 April 2016. Disease-associated glycans on cell surface proteins. Mol Aspects Med https://doi.org/10.1016/j.mam.2016.04.008.
14. Janik ME, Litynska A, Vereecken P. 2010. Cell migration—the role of integrin glycosylation. Biochim Biophys Acta 1800:545–555. https://doi.org/10.1016/j.bbagen.2010.03.013.
15. Hang Q, Isaji T, Hou S, Im S, Fukuda T, Gu J. 2015. Integrin alpha5 suppresses the phosphorylation of epidermal growth factor receptor and its cellular signaling of cell proliferation via N-glycosylation. J Biol Chem 290:29345–29360. https://doi.org/10.1074/jbc.M115.682229.
16. Mitra SK, Schlaepfer DD. 2006. Integrin-regulated FAK-Src signaling in normal and cancer cells. Curr Opin Cell Biol 18:516–523. https://doi.org/10.1016/j.ceb.2006.08.011.
17. Ginsberg MH, Partridge A, Shattil SJ. 2005. Integrin regulation. Curr Opin Cell Biol 17:509–516. https://doi.org/10.1016/j.ceb.2005.08.010.
18. Luque A, Gomez M, Puzon W, Takada Y, Sanchez-Madrid F, Cabanas C. 1996. Activated conformations of very late activation integrins detected by a group of antibodies (HUTS) specific for a novel regulatory region (355-425) of the common beta 1 chain. J Biol Chem 271:11067–11075. https://doi.org/10.1074/jbc.271.19.11067.
19. Arjonen A, Alanko J, Veltel S, Ivaska J. 2012. Distinct recycling of active and inactive beta1 integrins. Traffic 13:610–625. https://doi.org/10.1111/j.1600-0854.2012.01327.x.
20. Caswell PT, Norman JC. 2006. Integrin trafficking and the control of cell migration. Traffic 7:14–21. https://doi.org/10.1111/j.1600-0854.2005.00362.x.
21. Rankin CR, Hilgarth RS, Leoni G, Kwon M, Den Beste KA, Parkos CA, Nusrat A. 2013. Annexin A2 regulates beta1 integrin internalization and intestinal epithelial cell migration. J Biol Chem 288:15229–15239. https://doi.org/10.1074/jbc.M112.440909.
22. Streuli CH, Akhtar N. 2009. Signal co-operation between integrins and other receptor systems. Biochem J 418:491–506. https://doi.org/10.1042/BJ20081948.
23. Fiore VF, Ju L, Chen Y, Zhu C, Barker TH. 2014. Dynamic catch of a Thy-1-alpha5beta1+syndecan-4 trimolecular complex. Nat Commun 5:4886. https://doi.org/10.1038/ncomms5886.
24. Morgan MR, Hamidi H, Bass MD, Warwood S, Ballestrem C, Humphries MJ. 2013. Syndecan-4 phosphorylation is a control point for integrin recycling. Dev Cell 24:472–485. https://doi.org/10.1016/j.devcel.2013.01.027.
25. Tiwari S, Askari JA, Humphries MJ, Bulleid NJ. 2011. Divalent cations regulate the folding and activation status of integrins during their intracellular trafficking. J Cell Sci 124:1672–1680. https://doi.org/10.1242/jcs.084483.
26. Xu X, Nagarajan H, Lewis NE, Pan S, Cai Z, Liu X, Chen W, Xie M, Wang W, Hammond S, Andersen MR, Neff N, Passarelli B, Koh W, Fan HC, Wang J, Gui Y, Lee KH, Betenbaugh MJ, Quake SR, Famili I, Palsson BO, Wang J. 2011. The genomic sequence of the Chinese hamster ovary (CHO)-K1 cell line. Nat Biotechnol 29:735–741. https://doi.org/10.1038/nbt.1932.
27. Lu J, Gu J. 2015. Significance of beta-galactoside alpha2,6 sialyltranferase [*sic*] 1 in cancers. Molecules 20:7509–7527. https://doi.org/10.3390/molecules20057509.
28. Hood JD, Cheresh DA. 2002. Role of integrins in cell invasion and migration. Nat Rev Cancer 2:91–100. https://doi.org/10.1038/nrc727.
29. Wolfram T, Spatz JP, Burgess RW. 2008. Cell adhesion to agrin presented as a nanopatterned substrate is consistent with an interaction with the extracellular matrix and not transmembrane adhesion molecules. BMC Cell Biol 9:64. https://doi.org/10.1186/1471-2121-9-64.
30. DiMilla PA, Stone JA, Quinn JA, Albelda SM, Lauffenburger DA. 1993. Maximal migration of human smooth muscle cells on fibronectin and type IV collagen occurs at an intermediate attachment strength. J Cell Biol 122:729–737. https://doi.org/10.1083/jcb.122.3.729.
31. Parsons JT, Horwitz AR, Schwartz MA. 2010. Cell adhesion: integrating cytoskeletal dynamics and cellular tension. Nat Rev Mol Cell Biol 11:633–643. https://doi.org/10.1038/nrm2957.
32. Kinbara K, Goldfinger LE, Hansen M, Chou FL, Ginsberg MH. 2003. Ras GTPases: integrins' friends or foes? Nat Rev Mol Cell Biol 4:767–776. https://doi.org/10.1038/nrm1229.
33. Sheetz MP. 2001. Cell control by membrane-cytoskeleton adhesion. Nat Rev Mol Cell Biol 2:392–396. https://doi.org/10.1038/35073095.
34. Park EJ, Mora JR, Carman CV, Chen J, Sasaki Y, Cheng G, von Andrian UH, Shimaoka M. 2007. Aberrant activation of integrin alpha4beta7 suppresses lymphocyte migration to the gut. J Clin Invest 117:2526–2538. https://doi.org/10.1172/JCI31570.
35. Valdembri D, Caswell PT, Anderson KI, Schwarz JP, Konig I, Astanina E, Caccavari F, Norman JC, Humphries MJ, Bussolino F, Serini G. 2009. Neuropilin-1/GIPC1 signaling regulates alpha5beta1 integrin traffic and function in endothelial cells. PLoS Biol 7:e25. https://doi.org/10.1371/journal.pbio.1000025.
36. Bass MD, Williamson RC, Nunan RD, Humphries JD, Byron A, Morgan MR, Martin P, Humphries MJ. 2011. A syndecan-4 hair trigger initiates wound healing through caveolin- and RhoG-regulated integrin endocytosis. Dev Cell 21:681–693. https://doi.org/10.1016/j.devcel.2011.08.007.
37. Hines JH, Abu-Rub M, Henley JR. 2010. Asymmetric endocytosis and remodeling of beta1-integrin adhesions during growth cone chemorepulsion by MAG. Nat Neurosci 13:829–837. https://doi.org/10.1038/nn.2554.
38. Caswell PT, Chan M, Lindsay AJ, McCaffrey MW, Boettiger D, Norman JC. 2008. Rab-coupling protein coordinates recycling of alpha5beta1 integrin and EGFR1 to promote cell migration in 3D microenvironments. J Cell Biol 183:143–155. https://doi.org/10.1083/jcb.200804140.
39. Paszek MJ, DuFort CC, Rossier O, Bainer R, Mouw JK, Godula K, Hudak JE, Lakins JN, Wijekoon AC, Cassereau L, Rubashkin MG, Magbanua MJ, Thorn KS, Davidson MW, Rugo HS, Park JW, Hammer DA, Giannone G, Bertozzi CR, Weaver VM. 2014. The cancer glycocalyx mechanically primes integrin-mediated growth and survival. Nature 511:319–325. https://doi.org/10.1038/nature13535.
40. Palecek SP, Loftus JC, Ginsberg MH, Lauffenburger DA, Horwitz AF. 1997. Integrin-ligand binding properties govern cell migration speed through cell-substratum adhesiveness. Nature 385:537–540. https://doi.org/10.1038/385537a0.